M2 Muscarinic Receptor Activation Regulates Schwann Cell Differentiation and Myelin Organization

Carolina Uggenti,[1,2] M. Egle De Stefano,[1,2,3] Michele Costantino,[1,2] Simona Loreti,[1] Annalinda Pisano,[1] Bice Avallone,[4] Claudio Talora,[5] Valerio Magnaghi,[6] Ada Maria Tata[1,2]

[1] Dipartmento di Biologia e Biotecnologie "Charles Darwin," "Sapienza" Università di Roma, Roma, Italy

[2] Centro di ricerca in Neurobiologia "Daniel Bovet," "Sapienza" Università di Roma, Roma, Italy

[3] Istituto Pasteur-Fondazione Cenci Bolognetti, "Sapienza" Università di Roma, Italy

[4] Dipartimento di Biologia, Università "Federico II," Napoli, Italy

[5] Dip. di Medicina Molecolare, "Sapienza" Università di Roma, Roma, Italy

[6] Dip. di Scienze Farmacologiche e Biomolecolari, Università di Milano, Milano, Italy

Received 17 July 2013; revised 14 December 2013; accepted 15 December 2013

ABSTRACT: **Glial cells express acetylcholine receptors. In particular, rat Schwann cells express different muscarinic receptor subtypes, the most abundant of which is the M2 subtype. M2 receptor activation causes a reversible arrest of the cell cycle. This negative effect on Schwann cell proliferation suggests that these cells may possibly progress into a differentiating program. In this study we analyzed the *in vitro* modulation, by the M2 agonist arecaidine, of transcription factors and specific signaling pathways involved in Schwann cell differentiation. The arecaidine-induced M2 receptor activation significantly upregulates transcription factors involved in the promyelinating phase (e.g., Sox10 and Krox20) and downregulates proteins involved in the maintenance of the undifferentiated state (e.g., c-jun, Notch-1, and Jagged-1). Furthermore, arecaidine stimulation significantly increases the expression of myelin proteins, which is accompanied by evident changes in cell morphology, as indicated by electron microscopy analysis, and by substantial cellular re-distribution of actin and cell adhesion molecules. Moreover, ultrastructural and morphometric analyses on sciatic nerves of M2/M4 knockout mice show numerous degenerating axons and clear alterations in myelin organization compared with wild-type mice. Therefore, our data demonstrate that acetylcholine mediates axon-glia cross talk, favoring Schwann cell progression into a differentiated myelinating phenotype and contributing to compact myelin organization.** © 2013 Wiley Periodicals, Inc. Develop Neurobiol 74: 676–691, 2014

Keywords: **muscarinic receptors; acetylcholine; Schwann cells; transcription factors; myelin proteins**

INTRODUCTION

Large diameter axons are surrounded by myelin sheaths, which promote rapid conduction of nerve impulses and increase efficiency of nervous system communication. Myelin sheaths form during development and consist of compact spiral wraps of plasma membranes, which are supplied by oligodendrocytes

Additional Supporting Information may be found in the online version of this article.

Correspondence to: A.M. Tata (adamaria.tata@uniroma1.it).

Contract grant sponsor: Progetti di Ricerca "Sapienza," Universiy of Roma; contract grant number: C26A122HYC to (A.M.T.).

Contract grant sponsor: Association Francaise Contre les Myopathies; contract grant number: 14163/2012 (to V.M.).

Contract grant sponsor: ASI (Italian Space Agency) (to M.E.D.S.).

Published online 19 December 2013 in Wiley Online Library (wileyonlinelibrary.com).
DOI 10.1002/dneu.22161

(OLs) in the central nervous system (CNS) and by Schwann cells (SCs) in the peripheral nervous system (PNS). Myelinating glial cells and their target axons form intimate units, actively regulating each other's phenotype. During development, glial cells provide paracrine signals that support neuron survival and define both specific molecular domains on the axolemma and axonal diameter (Mirsky et al., 2008). In turn, axons provide signals regulating glial cell proliferation, survival, differentiation and myelin formation (Jessen and Mirsky, 2010; Taveggia et al., 2010).

Signals controlling SC development include several factors, such as endothelin, histamine and neuregulins (NRGs), and adhesion molecules (*N*-CAM, MAG, GAP-43) (Birchmeier and Nave, 2008; Woodhoo and Sommer, 2008). Some transcription factors, such as Sox10, Krox24, and Scip/Oct6, are also required for SC specification and remain active during their proliferation (Svaren and Meijer, 2008). When SCs begin to differentiate, the expression of the master regulator gene Sox10 increases and, in turn, upregulates Krox20 expression (Topilko et al., 1997). The concomitant increase in both transcription factors upregulates the expression of typical myelin-associated proteins, such as P0, the myelin basic protein (MBP) and PMP22 (Peirano et al., 2000; LeBlanc et al., 2006; Svaren and Meijer, 2008).

In adulthood, neuron-glia interactions are required to maintain axonal function and myelin integrity. In the PNS, axonal damage alters this relationship by promoting SC dedifferentiation, myelin reabsorption and axon regeneration. Dedifferentiation is the most relevant feature affecting myelinating SCs; in fact, in these conditions, these cells re-enter the cell cycle and acquire an immature phenotype (Jessen and Mirsky, 2005, 2008). This switch into a proliferative state represents an important step in the re-establishment of an environment favorable to nerve fiber regeneration. This dedifferentiation step is regulated by activation of c-jun and Notch-1 pathways (Arthur-Farraj et al., 2012; Fontana et al., 2012; Woodhoo et al., 2012).

Increasing evidences suggest that neurotransmitters can regulate neuron-glia cross-talk (Fields and Stevens-Graham, 2002; Loreti et al., 2007; Magnaghi et al., 2009). Glial cells express receptors for different neurotransmitters, indicating they might be involved in the modulation of glial cell survival, proliferation and differentiation (Magnaghi et al., 2004; Loreti et al., 2006). Acetylcholine (ACh) is an important neurotransmitter in both the CNS and PNS, whereas its additional function as a hormone has been described in several tissues, such as keratinocytes, lymphocytes and bronchial epithelia (Grando et al., 2006; Kawashima et al., 2004; Proskocil et al., 2004). Moreover, several studies indicate that muscarinic receptor activation modulates proliferation and survival of different glial cells, among which astrocytes and OLs (Murphy et al., 1986; Ragheb et al., 2001; De Angelis et al., 2012). We previously demonstrated that SCs are cholinoceptives, as they express several muscarinic ACh receptor subtypes. In particular, the expression of the M2 receptor is abundant and persists in mature SCs (Bernardini et al., 1999; Loreti et al., 2006, 2007). Activation of M2 receptors, by exposing cultured SCs to its agonist arecaidine, causes an arrest of SC proliferation. This block is reversible, as removing arecaidine from the culture medium enables SCs to recover their ability to proliferate (Loreti et al., 2007). These results prompted us to further investigate the involvement of M2 receptor activation in the modulation of SC differentiation. We, therefore, analyzed the effects of arecaidine treatment on the expression of several markers of SC differentiation (i.e., the TFs Sox10 and Krox20 and the myelin proteins P0, PMP22, and MBP) and dedifferentiation (i.e., c-jun, Notch-1, and Jagged-1). Our results show that M2 receptor activation upregulates promyelinating factors, which promote SC differentiation towards a myelinating phenotype, while it downregulates several factors involved in SC proliferation. The role of M2 receptors in myelin formation was also evaluated by transmission electron microscopy (TEM) and morphometric analysis of the sciatic nerve of M2/M4 knock-out mice.

MATERIALS AND METHODS

Ethics Statement

This study was carried out in accordance with the guidelines laid down by the European Community Council Directive 86/609/EEC of November 24, 1986. The protocol was approved by The Italian Ministry of Health. M2/M4 muscarinic receptor double knock-out mice were kindly provided by Dr. Jürgen Wess (NIH, Bethesda, MD).

Cell Cultures

SC primary cultures were obtained from sciatic nerves dissected from 2-day-old Wistar pups, according to the protocol described by Brockes (1987) and modified by Davis and Stroobant (1990). In brief, sciatic nerves were digested with trypsin/collagenase (Type I, Sigma-Aldrich, St. Louis, MA) and seeded into T25 flasks with fresh DMEM containing 10% fetal bovine serum (FBS, Sigma-Aldrich). To selectively remove fibroblasts, cells were treated with

Table 1 Primer Sequences Used in Real-Time PCR and RT-PCR Analysis

Gene	Forward 5′-3′	Reverse 5′-3′
Krox20/Egr2	TGTGGCACTTTAATGGCTTG	AGAACGAACGGAAGTGCAAT
Sox-10	ACTGGGAACAGCCAGTATATA	ACCAAACTCCTCCTTTGCCA
Jagged-1	ATGGCCTCCAACGATACTCCT	ACATGTACCCCCATAGTGGCA
Hes-1	GTCCCCGGTGGCTGCTAC	AACACGCTCGGGTCTGTGCT
c-jun	GATGGAAACGACCTTCTACGAC	AGCGTATTCTGGCTATGCAGTT
GAPDH	GTGCCAGCCTCGTCTCATAG	TGATGGCAACAATGTCCACT

1 m*M* cytosine arabinoside (AraC, Sigma-Aldrich) for 48 h and then with anti-Thy 1.1 (1:1000, Serotec, Bio-Rad group, Hercules, CA) and rabbit complement (1:2 v/v) (Cedarlane, ON, Canada). SCs were then amplified in DMEM, 10% FCS, 5 μ*M* forskolin (Fsk; Sigma-Aldrich) and bovine pituitary extract (1:150, Sigma-Aldrich), and maintained in DMEM, 10% FBS and 2 μ*M* Fsk during subsequent experiments.

Drug Treatments

SCs were incubated in the presence of the M2 selective agonist arecaidine (Sigma-Aldrich) (final concentration 100 μ*M*) (Loreti et al., 2007) for different times, according to the experimental plan (30 min, 1 h, 6 h, 24 h, and 48 h). Arecaidine is an alkaloid extracted from areca nuts; this type of alkaloids binds to all cholinergic receptors, but arecaidine acts as an agonist for atrial M2 muscarinic receptor (Barlow et al., 1985). Moreover, by pharmacological competition with selective M2 antagonists (gallamine or methoctramine) and silencing of M2 receptors by siRNAs, we have previously demonstrated that arecaidine is able to activate M2 receptor subtypes in different cell types (i.e., Schwann cells, OLs and glioblastoma cells) (Loreti et al., 2007; De Angelis et al., 2012; Ferretti et al., 2013).

Real-Time RT-PCR

Total RNA was extracted using Tri-reagent (Sigma-Aldrich) following manufacturer's instructions. Two micrograms of RNA from each sample were reverse transcribed for 60 min at 37°C with 1 μg of random hexamers (Promega Italia, Mi, Italy) as primers and 200 U of Moloney Murine Leukemia Virus (M-MLV) reverse transcriptase (Promega). Real-time Reverse Transcribed-Polymerase Chain Reaction (RT-PCR) analysis was performed by measuring the incorporation of SyBRGreen dye (Resnova, Genzano, RM, Italy) on the I Cycler IQ™ Multi-Color Real-Time PCR Detection system (Bio-Rad). The sequences of the primers used are reported in Table 1. Glyceraldehyde-3-phosphate dehydrogenase (GAPDH) was used as the internal control and all samples were run in triplicate. Results represent the mean of at least three independent experiments. Quantification was performed using the $2^{-\Delta\Delta Ct}$ method (Livak and Schmittgen, 2001).

Western Blot

Protein samples were extracted in either RIPA buffer (50 m*M* Tris-HCl pH 7.4, 150 m*M* NaCl, 1% NP40, 1× protease inhibitor cocktail, Sigma-Aldrich) or Laemmli sample buffer (Bio-Rad) with 20% β-mercaptoethanol (depending on the experimental plan). Samples were heated for 5 min at 95°C, loaded onto a 10% SDS polyacrylamide gel and run at 30 mA with running buffer (25 m*M* Tris, 190 m*M* glycine, 0.08% (w/v) SDS). SDS-PAGE gels were transferred overnight onto PVDF membranes (Millipore, Billerica, MA) at 37 V in transfer buffer (20 m*M* Tris; 150 m*M* glycine, 20% (v/v) methanol). Membranes were blocked in 5% non-fat dry milk (MARVEL, Dublin, Ireland) in phosphate buffered saline (PBS: 2.7 m*M* KCl, 137 m*M* NaCl, 1.5 m*M* KH_2PO_4, 9.2 m*M* Na_2HPO_4) before incubation with the primary antibody diluted in the blocking solution. Primary antibodies used were rabbit anti-P0 (1:200) (Sigma-Aldrich), rat anti-MBP (1:500) (Millipore), rabbit anti-c-jun (1:200) (Santa Cruz Biotechnology, Santa Cruz, CA), rabbit anti-Notch-1 (1:500) (Santa Cruz), rabbit anti-Cleaved Notch-1 (Val1744) (NICD) (1:500) (Cell Signaling, Boston, MA), rabbit anti-Sox10 (1:1000) (Millipore). Actin was used as the internal reference protein and detected by a rabbit anti-actin (1:1500) (Millipore). Membranes were incubated with appropriate HRP-conjugated secondary antibodies (1:20,000) (Promega) and antibody binding was revealed by using enhanced chemiluminescence (ECL) (Euroclone, Pero, Mi, Italy). The intensity of the bands was evaluated by densitometric analysis using the ImageQuant 5.2 program (Amersham Biosciences Europe, Cologno Monzese, Italy). The optical density (OD) of each protein band was normalized against the OD of the actin band. The ratios from at least three independent western blots were averaged and the standard error of the mean (SEM) calculated.

Immunocytochemistry

Schwann cells were plated onto 35-mm diameter dishes in complete DMEM, containing 10% FBS and 2 μ*M* forskolin, and maintained for 48 h in either the presence or absence of 100 μ*M* arecaidine. Cells were washed twice with PBS and fixed for 20 min in 4% paraformaldehyde in PBS, at room temperature (RT). After three washes in PBS, SCs were incubated for 45 min in 10% normal goat serum (NGS)

(Vector Laboratories, Burlingame, CA) and 1% bovine serum albumin (BSA) (Sigma-Aldrich) in PBS, and then overnight at 4°C with one of the following primary antibodies: rabbit anti-*N*-CAM (1:100) (Millipore) or mouse anti-*N*-cadherin (1:100) (Sigma-Aldrich), diluted in 1% NGS, 1% BSA in PBS. After two rinses (10 min each) in 1% BSA in PBS, SCs were incubated for 1 h at RT with the appropriate secondary antibodies: goat anti-rabbit IgG Alexa 488 or goat anti-mouse IgG Alexa 594 (Promega), diluted 1:250 in 1% BSA in PBS. After two rinses in 1% BSA in PBS, cultures were mounted with glycerol/PBS (3:1, v/v). Controls, obtained by omitting the primary antibody, were always immunonegative. Actin was visualized by using phalloidin-TRITC conjugated, diluted 1:50 in 1% BSA in PBS (Sigma) and nuclei were counterstained with Hoechst 33588.

Cell Infection with Adenovirus Expressing Notch-NICD

Recombinant adenoviruses expressing the constitutively active form of Notch-1 (NICD) and green fluorescent protein (GFP) were previously described (Rangarajan et al., 2001). Viruses were used at a multiplicity of infection of 50 MOI. SCs were infected with adeno-GFP and adeno-GFP-NICD for 1 h in a serum free medium, which was subsequently replaced with complete medium (10% FBS + 2 μ*M* Fsk). During the following days some plates were treated with arecaidine for 24 h and cells collected in Laemmli buffer (Bio-Rad) (100 μL/3 × 10^5 cells).

RNAse Protection Assay (RPA)

Samples containing 8 μg of total RNA were dissolved in 20 μL of hybridization solution (80% formamide, 40 m*M* PIPES, pH 6.4, 400 m*M* sodium acetate, pH 6.4, and 1 m*M* EDTA) containing 150,000 cpm of each ^{32}P-labeled cRNA probes and 50,000 cpm of ^{32}P-labeled cRNA 18 s probe. cRNA antisense probes were generated by *in vitro* transcription from pCR®II-TOP0® plasmids (Invitrogen, Life Technologies Italia, Monza, Italy) containing inserts specific for P0 and PMP22 mRNA and for 18 s rRNA (310 bp for P0, 415 bp for PMP22 and 290 bp for 18s rRNA). All cRNA probes had a specific activity $>10^8$ cpm/μg. After being heated at 85°C for 10 min, probes were hybridized overnight with the endogenous RNA at 45°C. Samples were then diluted with 200 μL of RNase digestion buffer (300 m*M* NaCl, 10 m*M* Tris-HCl pH 7.4, 5 m*M* EDTA pH 7.4), containing a cocktail of RNase (1 μg/μL RNase A and 20 U/μL RNase T1; Ambion Life Technologies Italia, Monza, Italy), diluted 1:400, and incubated for 30 min at 30°C. Ten micrograms of proteinase K (Ambion) and SDS (10 mL of a 20% stock solution) were added to samples and incubated at 37°C for 15 min. After incubation samples were extracted with phenol-chloroform and precipitated with ethanol. Pellets were dried and re-suspended in loading buffer (80% formamide, 0.1% xylene cyanol, 0.1% bromophenol blue, 2 m*M* EDTA), boiled at 95°C for 5 min and separated on a 5% polyacrilamide gel, under denaturing conditions (7*M* urea). The protected fragments were visualized by autoradiography and their size was determined by using ^{32}P-end labeled (T4 polynucleotide kinase) *MspI*-digested pBR322 fragments.

Light Microscopy and Morphometric Analysis of Sciatic Nerves

WT and M2/M4 knock-out (KO) mice were deeply anesthetized with a mixture of Zoletil (tiletamine chlorohydrate + zolazepam chlorohydrate, 25 mg/kg b.w.) (Virbac, France) and Rompun (xylazine, 8 mg/kg b.w.) (Bayer, Germany), and perfused transcardially with a Ca^{2+}-free oxygenated Ringer's variant, pH 7.3, followed by a fixative composed by 2% freshly depolymerized paraformaldehyde and 2.5% glutaraldehyde in 0.1*M* phosphate buffer (PB), pH 7.4. After fixation, sciatic nerves were dissected and placed in the same fixative overnight at 4°C. Following a rinse in PB, specimens were osmicated with 2% OsO_4 in 0.1*M* PB (1 h at 4°C), rinsed in distilled water, treated with aqueous 2% uranyl acetate (1 h at 4°C), rinsed again, dehydrated with a series of ascending ethyl alcohol and propylene oxide and embedded in Epon 812. Serial semithin sections (2 μm) were cut at an Reichert-Jung ultramicrotome (Leica), stained with 0.1% toluidine blue in 0.1% borax and permanently coverslipped with Eukitt balsam for light microscopy evaluation. Images were acquired with a Canon digital camera at 40× and then analyzed at a final magnification of 1500× using the Pro Plus Imaging software. For the morphometric investigation, we analyzed 4 WT and 4 M2/M4$^{-/-}$ mice, choosing three non-serial sections per animal. In each semithin section, 25 fields (corresponding to at least 50% of the total nerve cross-sectional area) were randomly selected (Mayhew and Sharma, 1984). Number, size, g-ratio (i.e., the ratio axon/fiber diameters) and the number of fibers with regular shapes (circularity index, IC > 0.75) were assessed on at least 500 myelinated fibers/section.

Transmission Electron Microscopy

From the same specimens used for semithin sections, ultrathin sections (50–60 nm) were cut, collected on single-hole Formvar-coated copper grids, counterstained with 2% uranyl acetate and 0.2% lead citrate, and viewed at an EM208S transmission electron microscope (TEM), operated at 80 kV. Images were acquired by a Megaview III camera and adjusted for contrast and brightness with Adobe Photoshop software.

Scanning Electron Microscopy

SCs adherent onto coverslips were fixed in 2% glutaraldehyde in 0.1*M* PBS pH 7.4, for 4 h at 4°C, and then rinsed overnight in PBS. The following day, samples were rinsed (3 × 15 min) in PBS 0.1*M* (pH 7.4) and post-fixed in 1%

OsO_4 in the same buffer for 1 h at 4°C. After a rinse (3 × 15 min) in 0.1*M* PBS, cells were dehydrated with a series of ascending ethanol alcohol and critical point dried in liquid CO_2. Samples were mounted on aluminum stubs and sputter coated with gold. The processed specimens were investigated and photographed using a JEOL 6700F SEM operated at 5 kV and an 8.3 mm working distance. Scanning Electron microscope (SEM) images were collected digitally.

Statistical Analysis

For both densitometric and morphometric analyses, one-way ANOVA and Bonferroni's multiple-comparisons post-hoc test were used to evaluate statistical significance between different experimental groups. Data were considered significant at $*p < 0.05$, $**p < 0.01$, and $***p < 0.001$.

RESULTS

M2 Receptor Activation Regulates Transcription Factors Modulating SC Development

The transition from promyelinating to myelinating SCs is regulated by several transcription factors, in particular Sox10 that, in turn, plays a critical role in the induction of the immediate early gene Krox20/Egr2. Therefore, we first investigated, by real-time RT-PCR, the expression level of *sox10* mRNA following stimulation with 100 μ*M* of M2 agonist arecaidine. M2 receptor activation induced a significant twofold increase in *sox10* mRNA after both 24 h and 48 h of treatment versus the control (without arecaidine) [Fig. 1(A)]. Upregulation of the *sox10* transcript matched a concomitant increase in the corresponding protein levels [Fig. 1(B), upper panel: representative western blot; lower panel: quantitative analysis]. *Sox10* transcript upregulation appears to depend directly on M2 receptor activation, as it was inhibited by incubating SCs with the M2 antagonist gallamine (10^{-6} M) (Supporting Information Fig. 1B; upper panel: representative RT-PCR; lower panel: densitometric analysis).

Since Krox20 is an immediate early gene potentially regulated also by Sox10, SCs were treated with arecaidine for short term (1 and 6 h) and *krox20* transcript levels were analyzed by real-time RT-PCR. As expected, *krox20* mRNA began to increase significantly, compared with untreated cells, after 30 min [Fig. 1(C)], with a transient peak (about 130-fold) at 1 h after arecaidine treatment [Fig. 1(C)]. Considering the ability of Krox20 to downregulate the expression of the transcription factor c-jun, implicated in the inhibition of SC differentiation and in the rescue of their proliferative activity (Parkinson et al., 2004), we also evaluated c-jun expression at both transcript and protein level following arecaidine treatment (100 μ*M*). After 1 h, *c-jun* transcript appeared to be downregulated when compared with untreated cells, as indicated by RT-PCR analysis [Fig. 2(A), representative RT-PCR; Fig. 2B, quantitative analysis]. By western blots, c-jun protein levels in untreated cells corresponded to an intense immunoreactive band of the predicted molecular mass [Fig. 2(C), first lane], which was consistent with the state of proliferating SCs (Arthur-Farraj, 2012). However, following stimulation with arecaidine, the expression of c-Jun significantly decreased after 24 h and disappeared after 48 h [Fig. 2(C), representative western blot; Fig. 2(D), densitometric analysis].

M2 Receptor Negatively Modulates Notch-1/Jagged-1 Pathway

Notch-1 signaling is involved in the regulation of transition from precursor to immature SCs and, together with c-jun, controls SCs plasticity and dedifferentiation after nerve injury (Woodhoo et al., 2009). Therefore, we investigated whether Notch-1 signaling was affected by the M2 agonist arecaidine. SC cultures were treated for 24 h with increasing concentrations of arecaidine (10, 50, and 100 μ*M*). No significant changes in SC morphology were observed after short-term arecaidine treatments [Fig. 3(A)]. Western blot analysis, performed in the same experimental conditions, showed that full-length Notch-1 expression was not modulated by arecaidine [Fig. 3(B), upper row of the representative Western blot shown in the upper panel], while expression of the active form of Notch (Notch Intracellular Domain; NICD) progressively decreased, reaching undetectable levels in cells treated with 100 μ*M* arecaidine [Fig. 3(B), lower row in the upper panel], which resulted in an almost fourfold decrease in the densitometry results when compared with control conditions [Fig. 3(B), lower panel]. To further validate these findings, we evaluated the expression of *hes-1*, the transcription factor downstream Notch signaling. As expected, real-time RT-PCR analysis showed a significant decrease in *hes-1* transcript levels following arecaidine treatment [Fig. 3(C)].

To investigate whether downregulation of the Notch-1 pathway was dependent on the expression of its specific ligands, we evaluated the expression of Delta-1 and Jagged-1. Delta-1 was not detectable in SCs *in vitro* (data not shown), but we found a consistent expression of Jagged-1 that was significantly

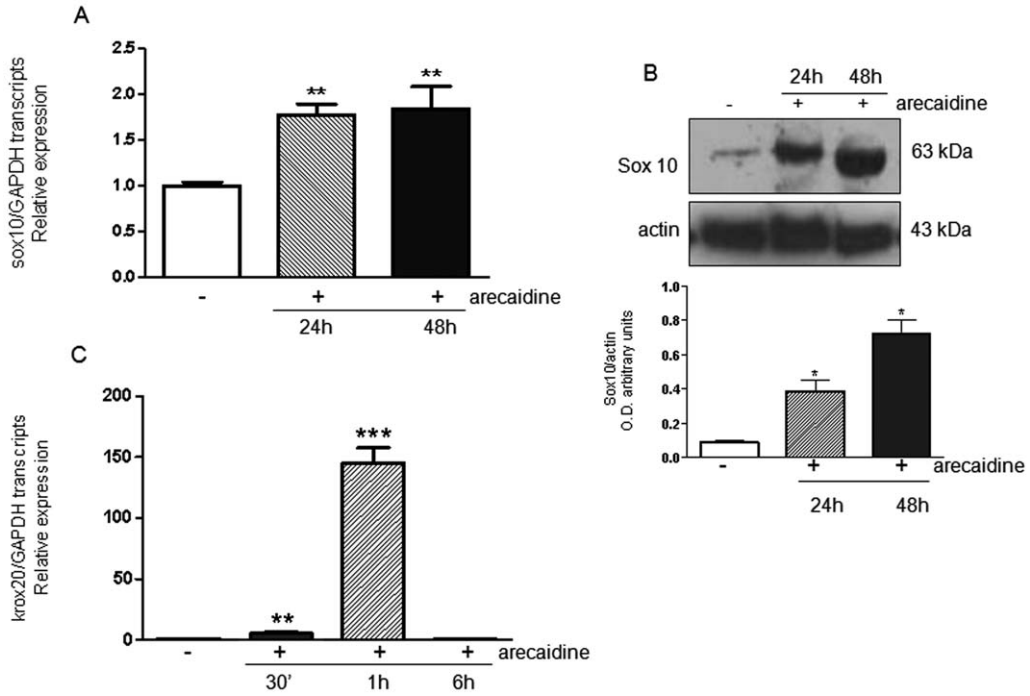

Figure 1 Sox10 and Krox20 expression in cultured SCs. A: Real-time RT-PCR analysis of sox10 expression in control and 100 μ*M* arecaidine-treated SCs (24 and 48 h). Transcript levels were normalized against the housekeeping gene GAPDH, and arecaidine-treated samples were normalized to control levels. B: Western immunoblot and densitometric analysis of Sox10 protein levels in control and 100 μ*M* arecaidine-treated SCs (24 and 48 h). In the upper panel, a representative western blot is shown. The graph below reports the densitometric analysis of Sox10 immunopositive bands. Actin was used as the internal reference protein. C: Real-time RT-PCR analysis of krox-20 expression in control and 100 μ*M* arecaidine-treated (30 min, 1 h, and 6 h) SCs. Transcript levels were normalized against the housekeeping gene GAPDH, and arecaidine-treated samples were normalized to control. Data represent the mean ± SEM of at least three independent experiments; $^{**}p < 0.01$; $^{***}p < 0.001$, by ANOVA and Bonferroni's post-hoc test.

reduced 24 h after arecaidine treatment [Fig. 4(D) representative Western immunoblot; Fig. 4(E), densitometric analysis]. To evaluate whether decreased expression of Jagged-1 was controlled by M2 receptors directly or via Notch-1 activation, we infected SCs with a recombinant adenovirus expressing the construct GFP-NICD. Successful transfection was evaluated analyzing the presence of GFP signal at the fluorescence microscope [Fig. 4(A,B)]. Expression of Notch-1 was then evaluated by western immunoblot using an antibody that recognizes its carboxy-terminus, common to both active and inactive forms of Notch-1. Untreated cells expressed Notch-1 [Fig. 4(C), top left panel, first lane] and, as previously demonstrated, arecaidine did not modulate this expression [Fig. 4(C), top left panel, second lane]. When SCs were infected with the adenovirus containing the NICD fragment, an increase in Notch-1 expression, compared with uninfected cells, was observed [Fig. 4(C), top right panel, first lane]. Again, arecaidine was unable to modulate this expression [Fig. 4(C), top right panel, second lane]. Concerning Jagged-1 expression, we observed that in cells infected with the control vector adeno-GFP [Fig. 4(D), representative western blot; Fig. 4(F), densitometric analysis], arecaidine treatment induced a decrease in protein expression similar to that observed in uninfected cells (control) [Fig. 4(D,E)]. Conversely, when SCs were infected with the adeno-GFP-NICD, no difference in Jagged-1 expression was observed after arecaidine treatment [Fig. 4(D,F)], suggesting that expression of Jagged-1 was directly controlled by Notch-1.

M2 Receptor Activation Induces Morphological Changes in SCs

When SCs arrest their proliferation and begin to differentiate, they undergo significant changes in cell

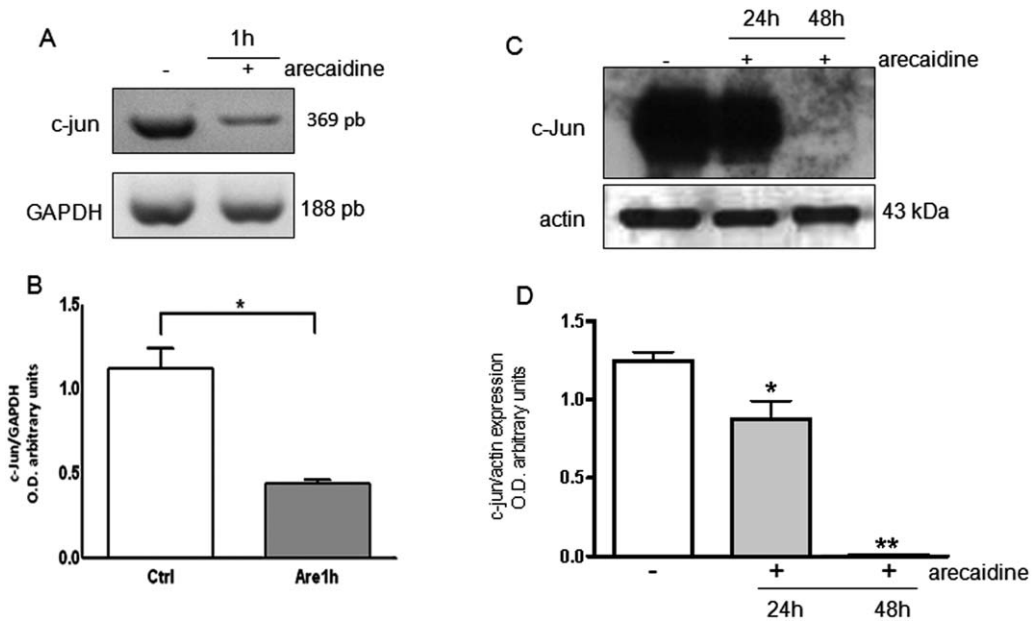

Figure 2 c-jun expression in cultured SCs. (A,B) RT-PCR analysis of c-jun transcript levels in control and 100 μ*M* arecaidine-treated SCs (1 h) (A), and relative densitometric analysis (B). Levels of mRNA transcripts were normalized against the housekeeping gene GAPDH, and arecaidine-treated samples were normalized to control. (C,D) Western blot analysis of c-Jun protein levels in control and 100 μ*M* arecaidine-treated SCs (24 and 48 h) (C), and relative densitometric analysis (D). Actin was used as internal reference protein. Data represent the mean ± SEM of at least three independent experiments; $*p < 0.05$; $**p < 0.01$, by ANOVA and Bonferroni's post-hoc test.

morphology due to modification of cytoskeletal organization and differential expression and/or distribution of adhesion molecules (Morgan et al., 1991; Fernandez-Valle, 1997; Li et al., 2003). To confirm the role of M2 signaling on SC differentiation, we evaluated morphological changes in SCs cultured in the absence or presence of arecaidine. As observed by SEM, when SCs were cultured in DMEM with addition of forskolin, a condition that promotes cell proliferation (Kim et al., 1997; Monje et al., 2006), they showed a classic bipolar morphology [Fig. 5(A,B)]. However, in these experimental conditions, some photographic fields showed several cells with a rounded morphology, typically associated to cells that enter the mitotic phase [see box in Fig. 5(A)]. Conversely, according with our previous data (Loreti et al., 2007), when SCs were cultured in the presence of arecaidine (100 μ*M*) for 48 h, they arrested their proliferation and appeared as flat cells juxtaposed to one another [Fig. 5(C,D)]; in this experimental condition the presence of "rounded morphology cells" was lacking. Although SCs changed their morphology after arecaidine treatment, the expression of SC markers (i.e., GFAP, S100*β*, p75) remained unmodified (see Supporting Information Fig. 3).

Due to these findings, we next assessed the expression and distribution of adhesion molecules such as *N*-CAM and *N*-cadherin. Albeit *N*-CAM was expressed at low levels, both proteins were distributed similarly in untreated cells, as observed by immunocytochemical analysis [Fig. 5(G,I)]. After 48 h of arecaidine treatment, both adhesion molecules clustered in restricted areas of contact between neighboring cells [Fig. 5(H,L)]. Similarly, in untreated cells actin filaments appeared organized to form stress fibers, which re-distributed under the plasma membrane following arecaidine treatment [Fig. 5(E,F)].

M2 Receptor Regulates SC Myelination

To confirm the ability of the M2 agonist arecaidine to modulate SC differentiation towards a myelinating phenotype, we analyzed the expression of several myelin proteins, namely P0, PMP22, and MBP. As expected, muscarine (100 μ*M*), a non-selective muscarinic agonist, induced a faint increase in the PMP22 transcript, but not in the P0 one. On the other hand, arecaidine (100 μ*M*) induced a strong increase in both P0 and PMP22 mRNAs [Fig. 6(A,B),

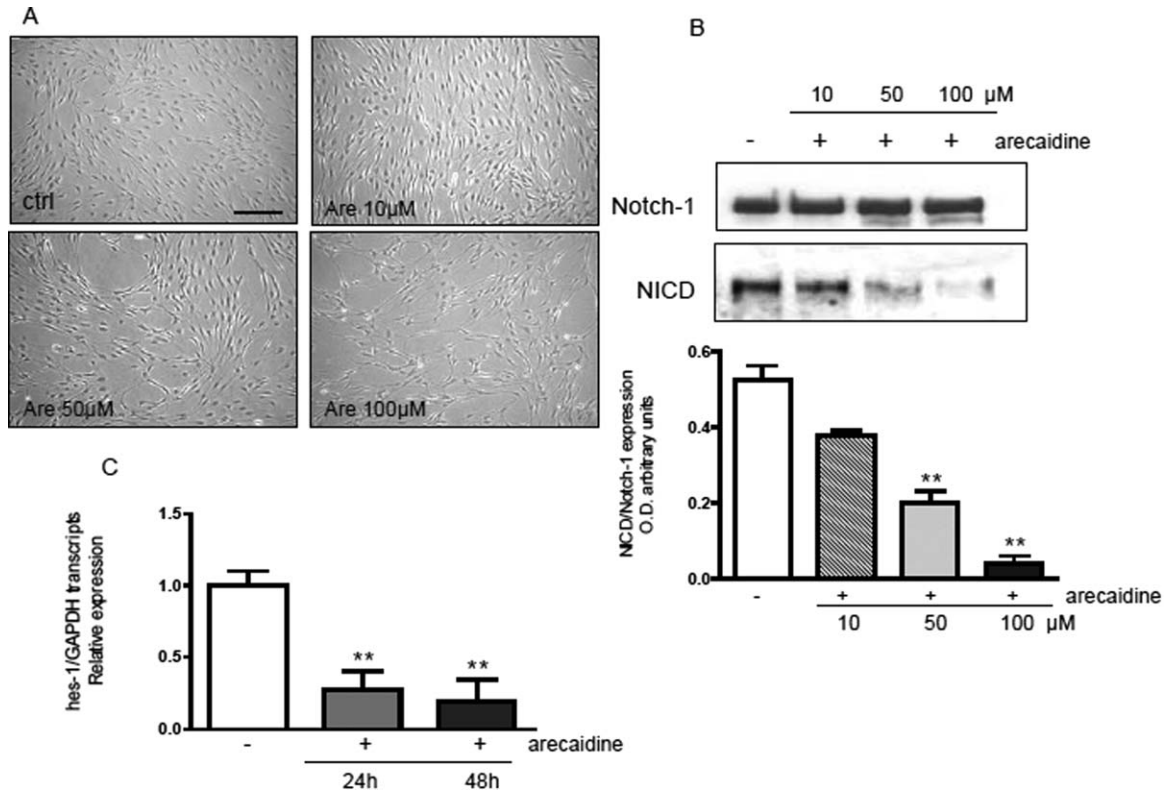

Figure 3 Activation of the Notch-1 pathway. A: SCs maintained *in vitro* in the absence (control) or in the presence of 10, 50, or 100 μ*M* arecaidine for 24 h (scale bar = 100 μ*M*). B: Western blot analysis of full length-Notch-1 and Notch-NICD protein levels in control and arecaidine-treated (10, 50, or 100 μ*M*) SCs. Representative western blots and relative densitometric analyses are shown in the upper and lower panel, respectively. Full-length Notch was used as the internal reference protein. C: Real-time RT-PCR analysis of hes-1 expression levels in control and 100 μ*M* arecaidine-treated SCs (24 and 48 h). Transcript levels were normalized against the housekeeping gene GAPDH and arecaidine-treated samples were compared with control. Data represent the mean ± SEM of at least three independent experiments; $^{**}p < 0.01$, by ANOVA and Bonferroni's post-hoc test.

densitometric analysis]. In agreement with these changes in mRNA expression, P0 and MBP protein levels increased after arecaidine treatment [Fig. 6(C), representative Western immunoblot; Fig. 6(D), densitometric analysis].

SC engagement into a myelinating phenotype was verified by both light and electron microscopy, and by morphometric analysis of toluidine blue stained semithin sections of sciatic nerve from double M2/M4$^{-/-}$ mice. When compared with wild type (WT), sciatic nerves from M2/M4$^{-/-}$ mice showed several alterations in myelin sheath organization of the medium/large-sized axons [Fig. 7(A), WT mice; Fig. 7(B), KO mice]. We identified three main types of morphological abnormalities: degenerating axons, myelin inclusions and loose myelin sheaths. These observations were supported by morphometric analysis, which underlined a significant increase in the number of degenerating axons and myelin inclusions, and an even more significant increase in the number of axons surrounded by loose myelin ($p < 0.001$, M2/M4$^{-/-}$ vs. WT) [Fig. 7(C)]. The area occupied by myelin sheath was also significantly increased in M2/M4$^{-/-}$ mice when compared with WT [Fig. 7(D)], possibly due to the presence of loose myelin, which contains large portions of cytoplasm not properly extruded [Fig. 7(E)].

TEM analysis confirmed the presence of myelin sheaths with different degrees of compactness (Fig. 8). Although myelin sheaths can assume bizarre configurations also in WT animals, several axons in M2/M4$^{-/-}$ mice displayed irregular and multi-lobed ensheathments, which intruded in the inner space occupied by the axon shaft itself. As a consequence, depending on the plane of cut, we could observe peculiar myelin figures, that is, circular multilamellar

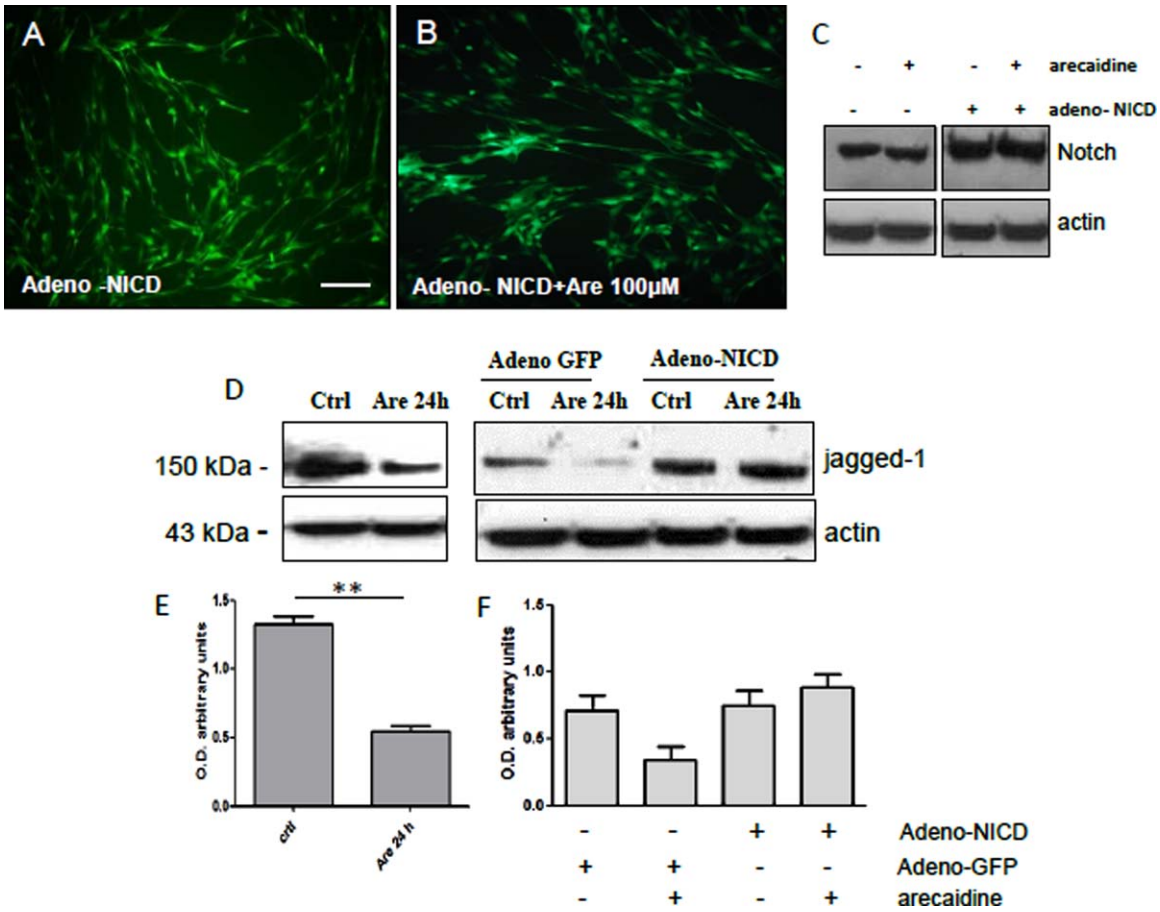

Figure 4 Overexpression of Notch-NICD in cultured SCs by adenovirus infection. (A,B) Representative fluorescence microscope images showing adenovirus-infected SCs expressing the GFP-NICD construct in control conditions (A) and after 100 μ*M* arecaidine treatment (24 h) (B) (scale bar = 50 μm). (C) Western immunoblot analysis of Notch-1 protein levels in control and 100 μ*M* arecaidine-treated (24 h) SCs, without adenoviral infection and 1 h after infection with the GFP-Notch/NICD adenovirus (with or without 100 μ*M* arecaidine treatment for 24 h). Notch protein levels increased in infected cells. (D) Representative western blot analysis of Jagged-1 protein levels in SCs maintained in control conditions (10% FBS+ 2 μ*M* fsk) without adenovirus or infected with the adenovirus-GFP only, or treated with the adenovirus GFP-NICD, in the absence or presence of 100 μ*M* arecaidine, for 24 h. (E) Densitometric analysis of the bands immunopositive for Jagged-1 in protein extracts from control SCs (without infection); (F) densitometric analysis of the bands immunopositive for Jagged-1 in protein extracts from SCs infected with either the adenovirus-GFP or the adenovirus GFP-NICD constructs. Actin was used as the internal reference protein. Data represent the mean ± SEM of at least three independent experiments; $^{**}p < 0.01$, by ANOVA and Bonferroni's post-hoc test. [Color figure can be viewed in the online issue, which is available at wileyonlinelibrary.com.]

bodies seemingly floating within the axoplasm [Fig. 8(A)]. In other axons, clear signs of progressive myelin sheath disorganization and degeneration were observed, which eventually led to axon degeneration and death. In Figure 8(B–G), we show a possible sequence of this SC-axon degeneration process: a) myelin sheath decompacting and presence of intercalating portions of cytoplasm between the lamellae [Fig. 8(B)]; b) signs of degeneration, with accumulation of cellular debris within the cytoplasm, while axons detach from myelin and are pushed aside [Fig. 8(C)]; c) axon caliber progressively reduces, while myelin sheaths decrease in thickness, subdividing in different compartments [Fig. 8(D)], until complete degeneration of both SC and axons occurs [Fig. 8(E–G)]. Other atypical aspects observed were abnormally thick myelin sheaths [Fig. 8(H)], which seemed to suffocate the inner axons until they degenerated

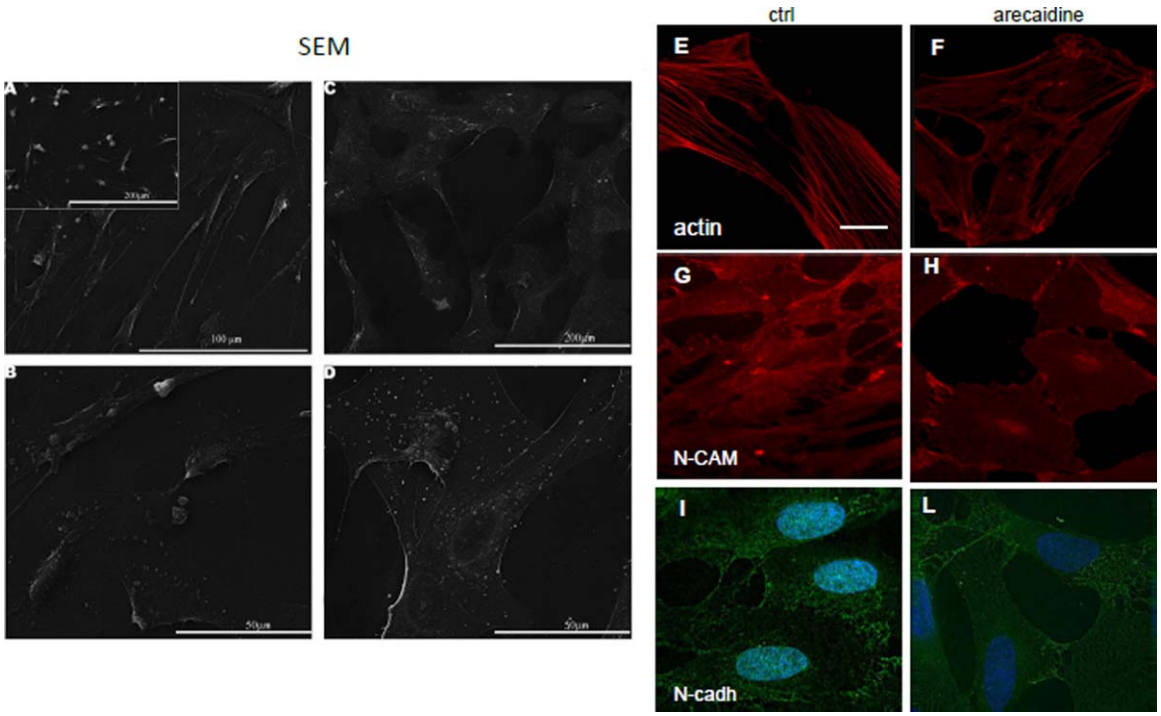

Figure 5 Morphological analysis by SEM of SCs maintained in control condition (10% FBS + 2 μ*M* fsk) (A,B) and after 48 h treatment with 100 μ*M* arecaidine (C,D). The box in panel (A) shows a representative field of untreated cells in active mitosis. (E,F) SC actin staining with phalloidin-TRITC conjugate in control conditions (E) and after treatment with 100 μ*M* arecaidine (F), showing redistribution of actin stress fibers after M2 agonist induction. (G–L) Immunocytochemistry for *N*-CAM (G,H) and *N*-caderin (*N*-cad, I,L) in control condition (10% FBS + 2 μ*M* fsk) (G,I) and after 100 μ*M* arecaidine treatment (48 h) (H,L). After treatment, both adhesion molecules aggregated in discrete areas at cell–cell points of contact (scale bar = 15 μm). [Color figure can be viewed in the online issue, which is available at wileyonlinelibrary.com.]

[Fig. 8(I)]. Axons displaying apparently healthy myelin sheaths could have eventually undergone degeneration, characterized by progressive axoplasm compaction. Nonetheless, as evidenced by light microscopy, numerous axons also displayed healthy myelin sheaths [Fig. 8(J)], as those seen in WT mice.

DISCUSSION

Development of SCs strictly depends on their interactions with neuronal axons. Although members of the NRG family have been described as the main regulatory molecules controlling the SC switch from a proliferative to a myelinating phenotype (Syed et al., 2010; Arthur-Farray et al., 2011), several evidences suggest that NRG signals alone are not sufficient (Jessen and Mirsky, 2010; Arthur-Farraj et al., 2011). Moreover, transcription factors ruling SC proliferation and differentiation have been largely described (Parkinson et al., 2004; Woodhoo et al., 2009; Doddrell et al., 2012; Fontana et al., 2012).

An important role of neurotransmitters in the control of neuron-glia cell interactions in both CNS and PNS is emerging. Several neurotransmitters, that is, GABA, ATP and adenosine, have been demonstrated to be involved in the modulation of glial cell physiology (Stevens et al., 2002; Magnaghi et al., 2004; Procacci et al., 2013). Among these, also ACh could play a role, since expression of different ACh receptors has been reported in different types of glial cells (OLs, astrocytes and SCs) (Murphy et al., 1986; Ragheb et al., 2001; Loreti et al., 2006; De Angelis et al., 2012). In this context, we demonstrated before that ACh controls OL and SC proliferation through activation of M3 and M2 muscarinic receptors, respectively (Loreti et al., 2007; De Angelis et al., 2012). In particular, we showed that activation of the M2 receptor in SCs (the most abundant receptor subtype expressed in these cells) with the agonist arecaidine, caused a reversible arrest of cell cycle progression, with accumulation of SCs in the G1 phase (Loreti et al., 2007). The effect of arecaidine could be counteracted by gallamine, an antagonist of

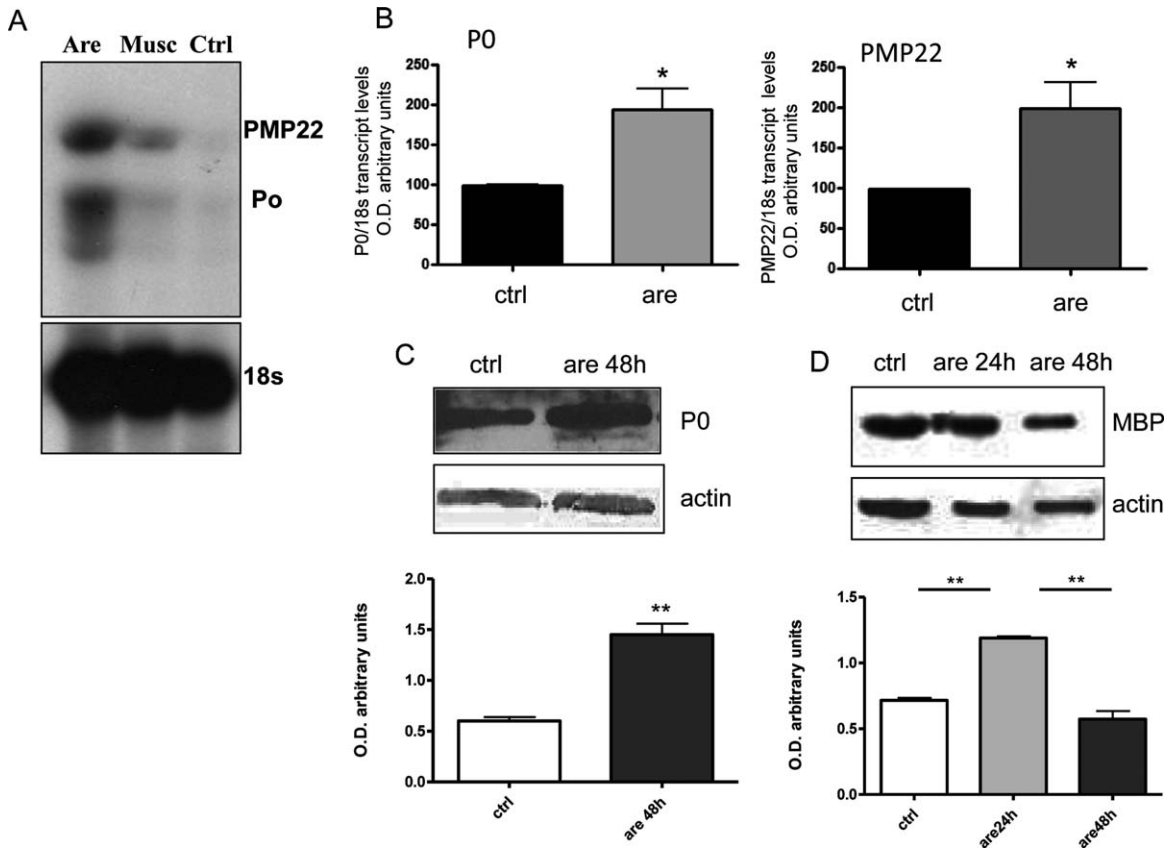

Figure 6 A: Expression of myelin mRNA transcripts for the PMP22 and P0 proteins in SCs maintained in the absence or presence of 100 μ*M* arecaidine (24 h). P0 and PMP22 mRNA levels were analyzed by RNAse protection assay. 18S was used as the housekeeping gene. B: Densitometric analysis of P0 and PMP22 mRNA expression. The intensity of the PM22 and P0 bands was normalized against that of 18 s. C: Western blot (upper panel) analysis of P0 protein levels in SCs maintained in the absence or in the presence 100 μ*M* arecadine (48 h) and relative densitometric analysis (lower panel). D: Western blot (upper panel) analysis of MBP protein levels in SCs maintained in the absence or in the presence 100 μ*M* arecaidine (24 h and 48 h) and relative densitometric analysis (lower panel). Actin was used as the internal reference protein. Data represent the mean ± SEM of at least three independent experiments; $*p < 0.05$, $**p < 0.01$, by ANOVA and Bonferroni post-hoc test.

the M2 receptor. In fact, co-treatment of SCs with gallamine and arecaidine rescued cell proliferation, demonstrating that arecaidine-mediated effects were dependent on M2 receptor activation (Loreti et al., 2007). Considering the ability of SCs to switch from a proliferative to a differentiated phenotype, a phenomenon that occurs during development and nerve fiber repair, we investigated whether blocking cell proliferation with the M2 agonist arecaidine could also modulate SC differentiation. To test this hypothesis, we evaluated the expression of some transcription factors involved in SC differentiation (i.e., Krox20 and Sox10) or proliferation (i.e., c-jun, Notch-1). Sox10 and Krox20/egr-2 have been identified as main transcriptional regulators of the myelination process. Although Sox10 was expressed early during SC proliferation, its increased levels may regulate cell entry in a promyelinating stage (Svaren and Meijer, 2008). The expression of these transcription factors was evaluated in SC cultured in either absence or presence of arecaidine (100 μ*M*). Short-term arecaidine stimulation (30 min or 1 h) had no effect on the levels of *sox10* transcript (Supporting Information Fig. 1A). Arecaidine induced the upregulation of both Sox10 transcript and protein levels after prolonged treatments in a time-dependent manner (24 and 48 h). This increase was directly modulated by M2 receptor activation, as the M2 antagonist

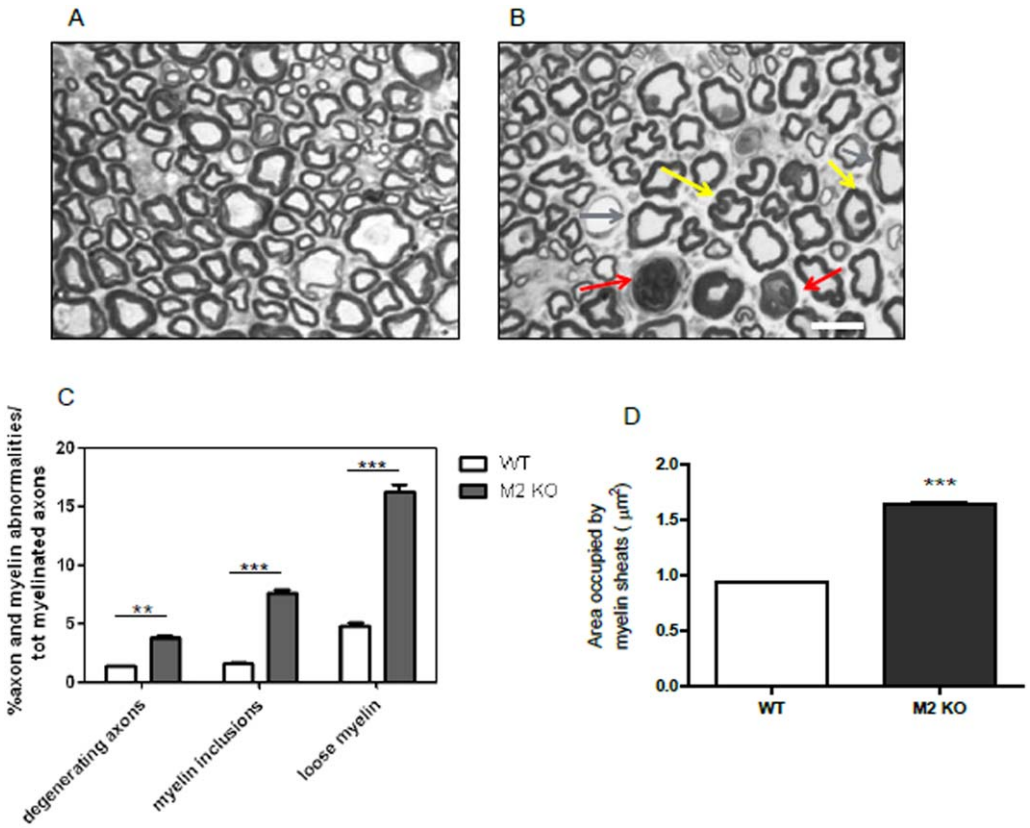

Figure 7 Semithin transverse sections (2-μm thick) of sciatic nerves of WT (A) and M2/M4$^{-/-}$ mice (B) stained with toluidine blue (scale bar = 15 μm). In KO mice, several morphological alterations in myelin organization and numerous degenerating axons are evident (red arrows: degenerating axons; yellow arrows: myelin inclusions; orange arrows: loose myelin). (C) Quantitative analysis of the most common morphological alterations observed in sciatic nerve semithin sections from WT and KO mice. The graph reports the percentage of degenerating axons, axons with myelin inclusions and axons with loose myelin. (D) Quantitative analysis of the area occupied by the myelin coat surrounding WT and KO mouse axons. Data represent the mean ± SEM; ***$p < 0.001$, **$p < 0.01$, by ANOVA and Bonferroni post-hoc test. [Color figure can be viewed in the online issue, which is available at wileyonlinelibrary.com.]

gallamine (10^{-6} M) counteracted the arecaidine-induced increase in *sox10* transcript (Supporting Information Fig. 1B).

In contrast, *krox20* was upregulated after 30 min of arecaidine treatment, further increased after 1 h ($p < 0.001$, 1 h arecaidine vs. control) and then rapidly decreased after 6 h, according to the typical pattern of induction of immediate early genes. After prolonged treatment with arecaidine (24 or 48 h), *krox20* mRNA was expressed in SCs, but its levels were not modified by M2 receptor activation (Supporting Information Fig. 2). Considering that members of the Krox(Egr) transcription factor family are enhanced by muscarinic receptor engagements (Ebihara and Saffen, 1997; von der Kammer et al., 1998; Salani et al., 2009), the early increase in Krox20 expression induced by arecaidine may depend on a direct regulation by M2 receptor activation rather than by Sox10 modulation. Although *krox20* mRNA expression is evident after prolonged arecaidine treatment, it did not increase as a consequence of the arecaidine-induced upregulation of Sox10 expression, suggesting that cholinergic stimulation alone may not be enough to sustain an extended activation of Krox20 in SCs.

Krox20 can modulate SC differentiation also by inducing cell cycle arrest, antagonizing c-jun expression (Parkinson et al., 2004). In fact, c-jun is typically downregulated in early post-natal SCs to allow myelination (Jessen and Mirsky, 2008), and it is rapidly upregulated after nerve injury, to promote an immature phenotype (De Felipe and Hunt, 1994; Stewart, 1995; Shy et al., 1996; Arthur-Farraj et al., 2012). As myelination is associated with c-jun downregulation,

and considering that early Krox20 upregulation was induced by arecaidine, we investigated the expression of c-jun after arecaidine stimulation. As expected, expression of the *c-jun* transcript was decreased 1 h after arecaidine treatment, while protein expression was reduced after 24 h and abolished after 48 h.

Krox20 is also able to downregulate Notch-1 expression (Taveggia et al., 2010). In the PNS Notch-

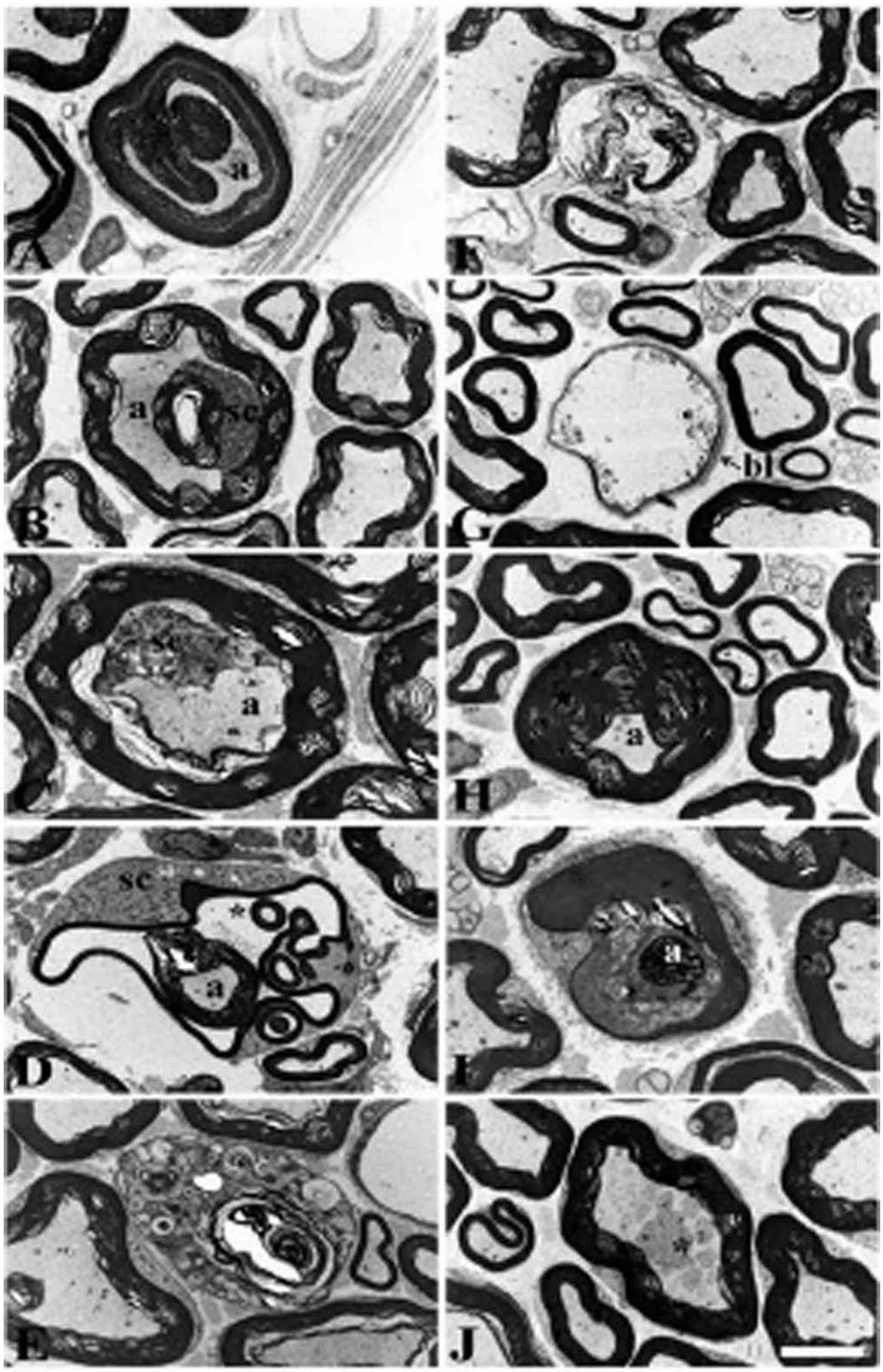

Figure 8

1 is expressed by SCs, whereas its ligand Jagged-1 is present in both SCs and axons. Notch-1 promotes SC transition from a precursor state to an immature phenotype (Woodhoo et al., 2009). As a matter of fact, overexpression of the active intracellular domain of Notch1 (NICD) delays myelination, while Notch-1 inactivation accelerates it (Woodhoo et al., 2009; Jessen and Mirsky, 2010). Analyzing Notch-1 and NICD expression in cultured SCs after arecaidine treatment, we observed that while the expression of full-length Notch-1 was not modulated, that of NICD was progressively reduced in a dose dependent manner. Recently, it has been demonstrated that, in myelinating SCs, Krox20 suppresses the formation of the NICD fragment (Woodhoo et al., 2009), suggesting that the observed arecaidine-induced NICD downregulation may be dependent on Krox20 activation.

In agreement with the decrease in NICD expression, we observed a decline in mRNA levels of *hes-1*, the canonical transcription factor downstream to the Notch pathway. Arecaidine treatment downregulated also the expression of Jagged-1, a ligand of Notch-1.

However, when the active form of Notch was overexpressed in SCs transduced with an adenovirus expressing the GFP-NICD fragment, we did not observe a downregulation of Jagged-1 after arecaidine treatment, compared with uninfected SCs and to cells infected with a control adenovirus containing a GFP-empty construct. In fact, Jagged-1 expression was unchanged after overexpression of the NICD fragment. These data suggest that the levels of Jagged-1 are directly controlled by Notch-1 and indirectly modulated by arecaidine, through NICD downregulation.

Activation of M2 cholinergic receptor, by positively regulating Sox10/Krox20 expression and antagonizing c-jun/Notch-1 activity, provides a molecular mechanism promoting the exit of SCs from the cell cycle, in agreement to our previous data (Loreti et al., 2007). To test the ability of M2 receptor to induce SC differentiation and considering that genes encoding myelin proteins, such as P0 and MBP, have consensus binding sites for Sox10 and Krox20 (Peirano et al., 2000; LeBlanc et al., 2005), we attempted to demonstrate that M2 receptor activation can also modulate myelin protein expression, at both transcriptional and post-transcriptional levels, possibly as a consequence of Sox10 and Krox20 upregulation. However, the increase in myelin protein expression, although significant, appeared modest. This may be in part dependent on the experimental conditions. In fact, when SCs are cultured *in vitro*, in the absence of axons, they are not able to achieve a complete myelination process because of lack of axon-derived signals (i.e., NRG1 Type III). Nevertheless, the increased levels of myelin proteins after arecaidine treatment may represent an initial signal of SC progression towards a myelinating phenotype and myelin organization.

This hypothesis is supported by our observations on M2/M4$^{-/-}$ mice. Sections of sciatic nerve from WT and M2/M4$^{-/-}$ mice, where M2 receptor signal transduction is absent, were analyzed for myelin organization. Since SCs do not express M4 receptors, as previously demonstrated (Loreti et al., 2006), we infer that the observed alterations mainly depend on the lack of M2 receptor signaling. Light and electron microscopic morphological analysis, along with morphometric evaluation of some axonal parameters, showed that, in KO mice, myelinated axons undergo significant alterations in myelin organization (e.g., myelin inclusions and loose myelin). In addition, SC treatment *in vitro* with arecaidine induced significant changes in cell morphology towards a differentiating phenotype, as evaluated by SEM analysis. This differentiation was accompanied by a re-arrangement of

Figure 8 Electron micrographs showing different degrees of SC-axon alteration in M2/M4 double KO mice. (A) Peculiar myelin conformation, in which the sheath repeatedly protrudes in the inner space occupied by the axon (a). The myelin sheath itself displays different degrees of compaction. (B) The myelin sheath has been divided in two by a large portion of Schwann cell cytoplasm (sc). (C) Schwann cell (sc) cytoplasm is starting to accumulate cellular debris, while the surrounded axon (a) has detached from myelin. (D) A Schwann cell (external cytoplasm indicated by sc) myelin sheath is dividing in thin layers formed by highly compact myelin separated by large empty spaces (asterisk), while the inner axon is reduced in caliber. (E) Degenerating Schwann cell (sc), for which a residue of the former myelin sheath is still present in the place of the degenerated axon. (F,G) Sites of degenerated Schwann cells and axons are identifiable by small remnants of a few loose myelin lamellae (F) and empty ghosts surrounded by the previous Schwann cell basal lamina (bl). (H) Small axon (a) surrounded by an abnormally thick myelin sheath. Surrounding axons appear normal. (I) Degenerated small axon surrounded by a thick-type myelin sheath with different degrees of compaction. (J) Large axon (a) with an apparently healthy myelin sheath, displays an initial collapse of the axoplasm (asterisk), presumably represented by compacted mitochondria. Scale bar: (C,I): 35 μm; (A,B,D–H,J): 50 μm.

actin stress fibers (evaluated by phalloidin labeling), which relocated under the plasma membrane, and a re-distribution of adhesion molecules (i.e., *N*-CAM and *N*-cadherin, evaluated by immunocytochemistry), which clustered in discrete areas where cell-to-cell contacts were formed. These dynamic changes indicate that both the cytoskeleton and adhesion molecules contribute to stabilize new myelinic structures (Fernadez-Valle et al., 1997; Tricaud et al., 2005).

Together, our data demonstrate that ACh represents an additional molecule active in regulating axon-SC cross-talk. As recently demonstrated, ACh can be released along cholinergic axons (Corsetti et al., 2012) and, therefore, contribute to the modulation of axon-ensheathing, SC proliferation and differentiation. Lack or low levels of ACh, together with high levels of NRG1, may favor SC proliferation, while high levels of ACh would arrest SC proliferation and direct them to a differentiation program towards a myelinating phenotype. The effect of the M2 agonist arecaidine on the block of SC proliferation is reversible (Loreti et al., 2007), further supporting the idea that ACh does not counteract SC plasticity, but may contribute to its modulation. This ability appears relevant not only during SC development, but also after cholinergic nerve injuries, where axon damage and the following reduction in ACh release may contribute to the rescue of SC proliferation.

The authors thank Dr. Jürgen Wess for the critical reading of the manuscript, Roberta Piovesana for technical assistance, and Dr. M.E. Miranda for English revision.

REFERENCES

Arthur-Farraj P, Wanek K, Hantke J, Davis CM, Jayakar A, Parkinson DB, Mirsky R, et al. 2011. Mouse schwann cells need both NRG1 and cyclic AMP to myelinate. Glia 59:720–733.

Arthur-Farraj PJ, Latouche M, Wilton DK, Quintes S, Chabrol E, Banerjee A, Woodhoo A, et al. 2012. c-Jun reprograms Schwann cells of injured nerves to generate a repair cell essential for regeneration. Neuron 75:633–647.

Barlow RB, Weston-Smith P. 1985. The relative potencies of some agonists at M2 muscarinic receptors in guinea-pig ileum, atria and bronchi. Br J Pharmacol 85:437–440.

Bernardini N, Levey AI, Augusti-Tocco G. 1999. Rat dorsal root ganglia express m1-m4 muscarinic receptor proteins. J Peripher Nerv Syst 4:222–232.

Birchmeier C, Nave, KA. 2008. Neuregulin-1, a key axonal signal that drives Schwann cell growth and differentiation. Glia 56:1491–1497.

Brockes JP. 1987. Assay and isolation of glial growth factor from the bovine pituitary. Methods Enzymol 147:217–225.

Corsetti V, Mozzetta C, Biagioni S, Augusti Tocco G, Tata AM. 2012. The mechanisms and possible sites of acetylcholine release during chick primary sensory neuron differentiation. Life Sci 91:783–788.

Davis JB, Stroobant P. 1990. Platelet-derived growth factors and fibroblast growth factors are mitogens for rat Schwann cells. J Cell Biol 110:1353–1360.

De Angelis F, Bernardo A, Magnaghi V, Minghetti,L, Tata AM. 2012. Muscarinic receptor subtypes as potential targets to modulate oligodendrocyte progenitor survival, proliferation, and differentiation. Devel Neurobiol 72: 713–728.

De Felipe C, Hunt SP. 1994. The differential control of c-jun expression in regenerating sensory neurons and their associated glial cells. J Neurosci 14:2911–2923.

Doddrell RD, Dun XP, Moate RM, Jessen KR, Mirsky R, Parkinson DB. 2012. Regulation of Schwann cell differentiation and proliferation by the Pax-3 transcription factor. Glia 60:1269–1278.

Ebihara T, Haga T. 1997. [Acetylcholine receptor]. Tanpakushitsu Kakusan Koso 42:275–284.

Fernandez-Valle C, Gorman D, Gomez AM, Bunge MB. 1997. Actin plays a role in both changes in cell shape and gene-expression associated with Schwann cell myelination. J Neurosci 17:241–250.

Ferretti M, Fabbiano C, Di Bari M, Conte C, Castigli E, Sciaccaluga M, Ponti D, et al. 2013. M2 receptor activation inhibits cell cycle progression and survival in human glioblastoma cells. J Cell Mol Med 17:552–566.

Fields RD, Stevens-Graham B. 2002. New insights into neuron-glia communication. Science 298:556–562.

Fontana X, Hristova M, Da Costa C, Patodia S, Thei L, Makwana M, Spencer-Dene B, et al. 2012. c-Jun in Schwann cells promotes axonal regeneration and motoneuron survival via paracrine signaling. J Cell Biol 198: 127–141.

Grando, SA. 2006. Cholinergic control of epidermal cohesion. Exp Dermatol 15:265–282.

Jessen KR, Mirsky R. 2005. The origin and development of glial cells in peripheral nerves. Nat Rev Neurosci 6:671–682.

Jessen KR, Mirsky R. 2008. Negative regulation of myelination: Relevance for development, injury, and demyelinating disease. Glia 56:1552–1565.

Jessen KR, Mirsky R. 2010. Control of Schwann cell myelination. F1000 Biol Rep 2:19.

Kawashima K, Fujii T. 2004. Expression of non-neuronal acetylcholine in lymphocytes and its contribution to the regulation of immune function. Front Biosci 9:2063–2085.

Kim HA, DeClue JE, Ratner N. 1997. cAMP-dependent protein kinase A is required for Schwann cell growth: Interactions between the cAMP and neuregulin/tyrosine kinase pathways. J Neurosci Res 49:236–247.

LeBlanc SE, Jang SW, Ward RM, Wrabetz L, Svaren J. 2006. Direct regulation of myelin protein zero expression by the Egr2 transactivator. J Biol Chem 281:5453–5460.

LeBlanc SE, Srinivasan R, Ferri C, Mager GM, Gillian-Daniel AL, Wrabetz L, Svaren J. 2005. Regulation of cholesterol/lipid biosynthetic genes by Egr2/Krox20 during peripheral nerve myelination. J Neurochem 93:737–748.

Li Y, Gonzalez MI, Meinkoth JL, Field J, Kazanietz MG, Tennekoon, GI. 2003. Lysophosphatidic acid promotes survival and differentiation of rat Schwann cells. J Biol Chem 278:9585–9591.

Livak KJ, Schmittgen TD. 2001. Analysis of relative gene expression data using real-time quantitative PCR and the 2(-Delta Delta C(T)) Method. Methods 25:402–408.

Loreti S, Ricordy R, De Stefano ME, Augusti-Tocco G, Tata AM. 2007. Acetylcholine inhibits cell cycle progression in rat Schwann cells by activation of the M2 receptor subtype. Neuron Glia Biol 3:269–279.

Loreti S, Vilaro MT, Visentin S, Rees H, Levey AI, Tata AM. 2006. Rat Schwann cells express M1-M4 muscarinic receptor subtypes. J Neurosci Res 84:97–105.

Magnaghi V, Ballabio M, Cavarretta IT, Froestl W, Lambert JJ, Zucchi I, Melcangi RC. 2004. GABAB receptors in Schwann cells influence proliferation and myelin protein expression. Eur J Neurosci 19:2641–2649.

Magnaghi V, Procacci P, Tata AM. 2009. Chapter 15: Novel pharmacological approaches to Schwann cells as neuroprotective agents for peripheral nerve regeneration. Int Rev Neurobiol 87:295–315.

Mayhew TM, Sharma, AK. 1984. Sampling schemes for estimating nerve fibre size. I. Methods for nerve trunks of mixed fascicularity. J Anat 139 (Pt 1), 45–58.

Mirsky R, Woodhoo A, Parkinson DB, Arthur-Farraj P, Bhaskaran A, Jessen KR. 2008. Novel signals controlling embryonic Schwann cell development, myelination and dedifferentiation. J Peripher Nerv Syst 13:122–135.

Monje PV, Bartlett Bunge M, Wood PM. 2006. Cyclic AMP synergistically enhances neuregulin-dependent ERK and Akt activation and cell cycle progression in Schwann cells. Glia 53:649–659.

Morgan L, Jessen KR, Mirsky R. 1991. The effects of cAMP on differentiation of cultured Schwann cells: Progression from an early phenotype (04+) to a myelin phenotype (P0+, GFAP-, N-CAM-, NGF-receptor-) depends on growth inhibition. J Cell Biol 112:457–467.

Murphy S, Pearce B, Morrow C. 1986. Astrocytes have both M1 and M2 muscarinic receptor subtypes. Brain Res 364:177–180.

Parkinson DB, Bhaskaran A, Droggiti A, Dickinson S, D'Antonio M, Mirsky R, Jessen KR. 2004. Krox-20 inhibits Jun-NH2-terminal kinase/c-Jun to control Schwann cell proliferation and death. J Cell Biol 164:385–394.

Peirano RI, Goerich DE, Riethmacher D, Wegner M. 2000. Protein zero gene expression is regulated by the glial transcription factor Sox10. Mol Cell Biol 20:3198–3209.

Procacci P, Ballabio M, Castelnovo LF, Mantovani C, Magnaghi V. 2012. GABA-B receptors in the PNS have a role in Schwann cells differentiation? Front Cell Neurosci 6:1–7.

Proskocil BJ, Sekhon HS, Jia Y, Savchenko V, Blakely RD, Lindstrom J, Spindel ER. 2004. Acetylcholine is an autocrine or paracrine hormone synthesized and secreted by airway bronchial epithelial cells. Endocrinology 145: 2498–2506.

Ragheb F, Molina-Holgado E, Cui QL, Khorchid A, Liu HN, Larocca JN, Almazan G. 2001. Pharmacological and functional characterization of muscarinic receptor subtypes in developing oligodendrocytes. J Neurochem 77:1396–1406.

Rangarajan A, Talora C, Okuyama R, Nicolas M, Mammucari C, Oh H, Aster JC, et al. 2001. Notch signaling is a direct determinant of keratinocyte growth arrest and entry into differentiation. EMBO J 20:3427–3436.

Salani M, Anelli T, Tocco GA, Lucarini E, Mozzetta C, Poiana G, Tata AM, et al. 2009. Acetylcholine-induced neuronal differentiation: Muscarinic receptor activation regulates EGR-1 and REST expression in neuroblastoma cells. J Neurochem 108:821–834.

Shy ME, Shi Y, Wrabetz L, Kamholz J, Scherer SS. 1996. Axon-Schwann cell interactions regulate the expression of c-jun in Schwann cells. J Neurosci Res 43:511–525.

Stevens B, Porta S, Haak LL, Gallo V, Fields RD. 2002. Adenosine: A neuron-glial transmitter promoting myelination in the CNS in response to action potentials. Neuron 36:855–868.

Stewart, HJ. 1995. Expression of c-Jun, Jun B, Jun D and cAMP response element binding protein by Schwann cells and their precursors in vivo and in vitro. Eur J Neurosci 7:1366–1375.

Svaren J, Meijer D. 2008. The molecular machinery of myelin gene transcription in Schwann cells. Glia 56: 1541–1551.

Syed N, Reddy K, Yang DP, Taveggia C, Salzer JL, Maurel P, Kim HA. 2010. Soluble neuregulin-1 has bifunctional, concentration-dependent effects on Schwann cell myelination. J Neurosci 30:6122–6131.

Taveggia C, Feltri ML, Wrabetz L. 2010. Signals to promote myelin formation and repair. Nat Rev Neurol 6: 276–287.

Topilko P, Levi G, Merlo G, Mantero S, Desmarquet C, Mancardi G, Charnay P. 1997. Differential regulation of the zinc finger genes Krox-20 and Krox-24 (Egr-1) suggests antagonistic roles in Schwann cells. J Neurosci Res 50:702–712.

Tricaud N, Perrin-Tricaud C, Bruses JL, Rutishauser U. 2005. Adherens junctions in myelinating Schwann cells stabilize Schmidt-Lanterman incisures via recruitment of p120 catenin to E-cadherin. J Neurosci 25:3259–3269.

Von der Kammer H, Mayhaus M, Albrecht C, Enderich J, Wegner M, Nitsch RM. 1998. Muscarinic acetylcholine receptors activate expression of the EGR gene family of transcription factors. J Biol Chem 273:14538–14544.

Woodhoo A, Alonso MB, Droggiti A, Turmaine M, D'Antonio M, Parkinson DB, Wilton DK, et al. 2009. Notch controls embryonic Schwann cell differentiation, postnatal myelination and adult plasticity. Nat Neurosci 12:839–847.

Woodhoo A, Sommer L. 2008. Development of the Schwann cell lineage: From the neural crest to the myelinated nerve. Glia 56:1481–1490.